Calculations of the electronic properties of substoichiometric Ti-Fe hydride

D. A. Papaconstantopoulos
Naval Research Laboratory, Washington, D.C. 20375-5000

A. C. Switendick
Sandia Laboratories, Albuquerque, New Mexico 87185

(Received 16 August 1984)

We have calculated the electronic structure of $TiFeH_x$ using the tight-binding coherent-potential-approximation method. The tight-binding parameters were determined by Slater-Koster fits to augmented-plane-wave calculations of TiFe and $TiFeH_{1.0}$. We have computed the densities of states (DOS) for the hydrogen concentrations $x=0.1$, $x=0.8$, and $x=0.9$, and obtained the angular-momentum and site-decomposed DOS. We have found that the Fermi level E_F is very nearly independent of x, but the DOS values at E_F increase rapidly with x in agreement with experiment. We discuss various features of the DOS relating to the effects of hydrogenation and disorder.

I. INTRODUCTION

Electronic-structure calculations for binary-metal hydrides have clarified the change in the electronic structure of the (sometimes fictitious) host lattice upon the addition of hydrogen to form the hydride.[1-4] In the transition series these changes have been seen to be of three types: (1) the lowering of previously occupied states, (2) the introduction of new low-lying states, and (3) the lowering of states from above the Fermi level to below. All these modified states have s-like character about the hydrogen sites. Since the hydrogen-to-transition-metal ratios are from 0—3, this means that typically $\frac{4}{5}$ of the d states associated with canonical band structure of the transition-metal lattice are largely unaffected. The relative amounts of each of these changes vary from one host-crystal structure to another and even within the same or similar structures. Thus, it is unadvisable to generalize from limited results.

The simplest question one can ask is whether the Fermi level goes up or down, i.e., what are the relative proportions of distribution of the added hydrogen electrons between the latter two types of states mentioned above? One of the present authors,[1] based on comparisons of the band structures of the unhydrided host and the hydride, has estimated that the number of electrons per hydrogen added to the canonical host d states ranges from 0.4 for TiH_2 to 1.0 for CrH. Recent comparison of experimental data and detailed density of states (DOS) for TiH_x and ZrH_x ($1.6<x<2.0$) has yielded a value in the range of 0.50—0.75 electrons based on the dihydride band structures.[5] Similar estimates have been made by Chan and Louie[6] and by Temmerman and co-workers.[7]

In the search for hydrides for practical applications, cost and weight factors have ruled out any large-scale use of binary hydrides.[8] Thus, one is led to consider binary- and ternary-based metal alloy systems for hydrogen storage. Here the understanding is complicated by the introduction of the new component(s) which interacts both with the other component(s) and the hydrogen. In these cases, one has very little understanding of even the host band structure, and the situation becomes more complicated in that one may have disorder in the host or missing atoms on the hydrogen lattice (which exists even for binary hydrides).

Due to the complexity of the problem, investigators

TABLE I. Slater-Koster parameters for TiFe.

	Ti-Ti	Fe-Fe
$E_{s,s}(000)$	1.5836	1.1222
$E_{x,x}(000)$	1.3916	2.1064
$E_{xy,xy}(000)$	0.7727	0.6268
$E_{d2,d2}(100)$	0.7873	0.6018
$E_{s,s}(200)$	−0.0225	−0.0330
$E_{s,x}(200)$	−0.0683	0.2116
$E_{s,d2}(002)$	−0.0648	0.0448
$E_{x,x}(200)$	0.1507	0.3321
$E_{y,y}(200)$	−0.0598	0.0437
$E_{x,xy}(020)$	−0.0114	0.0648
$E_{z,d2}(002)$	−0.0262	−0.0709
$E_{xy,xy}(200)$	0.0185	0.0152
$E_{xy,xy}(002)$	−0.0130	0.0043
$E_{d2,d2}(002)$	−0.0483	−0.0264
$E_{d1,d1}(002)$	0.0062	−0.0002
	Ti-Fe	**Fe-Ti**
$E_{s,s}(111)$	0.1218	0.1218
$E_{s,x}(111)$	−0.0950	−0.0490
$E_{s,xy}(111)$	0.0138	−0.0373
$E_{x,x}(111)$	0.0344	0.0344
$E_{x,y}(111)$	0.0603	0.0603
$E_{x,xy}(111)$	−0.0198	0.0151
$E_{x,yz}(111)$	−0.0153	0.0426
$E_{x,d1}(111)$	−0.0085	−0.0714
$E_{xy,xy}(111)$	0.0163	0.0163
$E_{xy,xz}(111)$	0.0200	0.0200
$E_{xy,d2}(111)$	0.0125	0.0202
$E_{d2,d2}(111)$	−0.0207	−0.0207

 ©1985 The American Physical Society

have resorted to quasichemical or empirical approaches.[9–11] However, due to the development of the coherent-potential approximation[12] (CPA) more realistic calculations are now possible. Fortunately, two state-of-the-art calculations exist for one of the leading candidates for hydrogen storage, Ti-Fe. In an earlier work,[13] one of us calculated the electronic band structure of crystalline Ti-Fe in the cesium chloride structure, and Gupta,[14] in a pioneering calculation for Ti-Fe-H, has provided a benchmark for these types of ternary systems. We shall attempt to explore the physics for intermediate compositions using a tight-binding formalism of the CPA.[15,16] This work is an improvement, extension, and more complete discussion of an earlier work.[17]

II. SLATER-KOSTER INTERPOLATION FOR TiFe

We have performed a Slater-Koster[18] (SK) fit to the augmented-plane-wave (APW) calculations for TiFe in the CsCl structure.[13] This involves an 18×18 Hamiltonian consisting of the s-, p-, and d-like orbitals of both the Ti and Fe sites. To avoid incorrect assignments of states we used group theory to reduce the 18×18 matrix to smaller matrices at high-symmetry points or lines in the Brillouin zone.[19] We utilized 48 three-center-integral parameters that included up to second-neighbor interactions. In our earlier calculations,[17] we had included the third-neighbor interactions, which increased the number of parameters to 82. However, we found that 48 parameters fit the bands just as well as 82 parameters. In fact, by improving our least-squares computer code we have now obtained a better fit with 48 parameters than we did before with 82 parameters. We performed a fit to the APW results at 16 k points in the irreducible Brillouin zone, while we have taken a rms error at 35 k points. The rms fitting error was less than 10 mRy for 11 bands. The SK parameters are listed in Table I.

III. SLATER-KOSTER INTERPOLATION FOR TiFeH

The compound $TiFeH_{1.0}$ has the orthorhombic structure that results from the doubling of the CsCl unit cell of

TABLE II. Matrix elements involving hydrogen interactions with Ti and Fe. h_1 and h_2 indicate the two hydrogen atoms in the 38×38 matrix and the indices 1 and 2 on the left denote Ti and Fe, respectively. The notation is that of Ref. 18.

$(h_1 \mid h_1)=(h_2 \mid h_2)$	$E_{h,h}(000)+2E_{h,h}(200)\cos(2x)$
$(h_1 \mid h_2)$	$2E_{h,h}(011)\cos(z-y)$
$(s_1^+ \mid h_1)$	$2\sqrt{2}E_{h,s}(110)\cos x\cos y$
$(x_1^+ \mid h_1)$	$2\sqrt{2}E_{h,x}(110)\sin x\cos y$
$(y_1^+ \mid h_1)$	$2\sqrt{2}E_{h,x}(110)\cos x\sin y$
$(z_1^+ \mid h_1)$	0
$(xy_1^+ \mid h_1)$	$-2\sqrt{2}E_{h,xy}(110)\sin x\sin y$
$(yz_1^+ \mid h_1)=(zx_1^+ \mid h_1)$	0
$[(x^2-y^2)_1^+ \mid h_1]$	0
$[(3z^2-r^2)_1^+ \mid h_1]$	$2\sqrt{2}E_{h,3z^2-r^2}(110))\cos x\cos y$
$(s_2^+ \mid h_1)$	$\sqrt{2}E_{h,s}(001)\cos z$
$(x_2^+ \mid h_1)=(y_2^+ \mid h_1)$	0
$(z_2^+ \mid h_1)$	$\sqrt{2}E_{h,z}(001)\sin z$
$(xy_2^+ \mid h_1)=(yz_2^+ \mid h_1)=(zx_2^+ /h_1)$	0
$[(x^2-y^2)_2^+ \mid h_1]$	0
$[(3z^2-r^2)_2^+ \mid h_1]$	$\sqrt{2}E_{h,3z^2-r^2}(001)\cos z$
$(s_1^+ \mid h_2)$	$2\sqrt{2}E_{h,s}(110)\cos x\cos z$
$(x_1^+ \mid h_2)$	$2\sqrt{2}E_{h,x}(110)\sin x\cos z$
$(y_1^+ \mid h_2)$	0
$(z_1^+ \mid h_2)$	$2\sqrt{2}E_{h,x}(110)\cos x\sin z$
$(xy_1^+ \mid h_2)=(yz_1^+ \mid h_2)$	0
$(zx_1^+ \mid h_2)$	$-2\sqrt{2}E_{h,xy}(110)\sin x\sin z$
$[(x^2-y^2)_1^+ \mid h_2]$	$-\sqrt{6}E_{h,3z^2-r^2}(110)\cos x\cos z$
$[(3z^2-r^2)_1^+ \mid h_2]$	$-\sqrt{2}E_{h,3z^2-r^2}(110)\cos x\cos z$
$(s_2^+ \mid h_2)$	$\sqrt{2}E_{h,s}(001)\cos y$
$(x_2^+ \mid h_2)=(z_2^+ \mid h_2)$	0
$y_2 \mid h_2$	$\sqrt{2}E_{h,z}(001)\sin y$
$(xy_2^+ \mid h_2)=(yz_2^+ \mid h_2)=(zx_2^+ \mid h_2)$	0
$[(x^2-y^2)_2^+ \mid h_2]$	$-\sqrt{3/2}E_{h,3z^2-r^2}(001)\cos y$
$[(3z^2-r^2)_2^+ \mid h_2]$	$-\sqrt{1/2}E_{h,3z^2-r^2}(001)\cos y$

TABLE III. Slater-Koster parameters for $TiFeH_{1.0}$.

	Ti-Ti	Fe-Fe
$E_{s,s}(000)$	1.9144	0.9140
$E_{x,x}(000)$	1.2862	2.0988
$E_{xy,xy}(000)$	0.8486	0.6213
$E_{d2,d2}(000)$	0.7720	0.6114
$E_{s,s}(200)$	0.1575	−0.0427
$E_{s,x}(200)$	−0.1180	0.1864
$E_{s,d2}(002)$	−0.0805	0.0415
$E_{x,x}(200)$	0.2122	0.3752
$E_{y,y}(200)$	−0.0205	0.0449
$E_{x,xy}(020)$	0.0346	0.0654
$E_{z,d2}(002)$	0.0246	−0.0248
$E_{xy,xy}(200)$	0.0140	0.0142
$E_{xy,xy}(002)$	−0.0333	−0.0038
$E_{d2,d2}(002)$	−0.0538	−0.0028
$E_{d1,d1}(002)$	−0.0109	0.0115
	Ti-Fe	Fe-Ti
$E_{s,s}(111)$	0.1030	0.1030
$E_{s,x}(111)$	−0.1002	−0.0368
$E_{s,xy}(111)$	−0.0120	−0.0425
$E_{x,x}(111)$	−0.0326	−0.0326
$E_{x,y}(111)$	0.0267	0.0267
$E_{x,xy}(111)$	−0.0261	0.0222

	Ti-Fe	Fe-Ti
$E_{x,yz}(111)$	−0.0231	0.0399
$E_{x,d1}(111)$	−0.0011	−0.0700
$E_{xy,xy}(111)$	0.0231	0.0231
$E_{xy,xz}(111)$	0.0177	0.0177
$E_{xy,d2}(111)$	0.0057	0.0159
$E_{d2,d2}(111)$	−0.0302	−0.0302
	H-H	
$E_{h,h}(000)$	1.6662	
$E_{h,h}(200)$	−0.0315	
$E_{h,h}(011)$	0.2193	
	H-Ti	
$E_{h,s}(110)$	0.1771	
$E_{h,x}(110)$	0.0206	
$E_{h,xy}(110)$	0.1363	
$E_{h,d2}(110)$	0.1230	
	H-Fe	
$E_{h,s}(001)$	0.5974	
$E_{h,z}(001)$	0.1400	
$E_{h,d2}(001)$	0.4155	

TiFe followed by the tetragonal and orthorhombic distortions. The band structure of $TiFeH_{1.0}$ has been calculated by Gupta[14] using the APW method. In order to fit this calculation, one must first double the size of the TiFe basis set to reflect the four transition-metal atoms in the new unit cell and add two hydrogen basis functions and their interactions with the transition metals so that the matrix becomes 38×38. Although one could derive the SK matrix for the orthorhombic structure, it is easier and more instructive to cast the problem in terms of the original SK matrix for cubic TiFe.[19] This is equivalent to taking $b=c=\sqrt{2}a_0$ where a_0 is the TiFe lattice constant. Thus, the matrix elements of the transition metals retain their x, y, and z cubiclike symmetry, but the interactions with (and between) the hydrogens are of true orthorhombic character. This pseudocubic structure differs at most by 8%, in a cell dimension, from the observed one. One can retain the original TiFe cesium chloride SK matrix by taking the appropriate linear combinations of the (now) two types of titanium and iron atoms in the unit cell

$$s^{+}_{\mathrm{Ti}}=[s_{\mathrm{Ti}}(0,a/2,0)+s_{\mathrm{Ti}}(0,-a/2,0)]/\sqrt{2},\ \ldots\ ,$$

and

$$s^{-}_{\mathrm{Fe}}=[s_{\mathrm{Fe}}(0,0,a/2)-s_{\mathrm{Fe}}(0,0,-a/2)]/\sqrt{2},\ldots\ .$$

These linear combinations also greatly simplify the transition-metal—hydrogen interactions.

We also note that by choosing the appropriate phases $(\pm i,\pm1)$ of the basis functions one can write the SK matrix without any complex elements by dropping the i in the (all imaginary) complex elements.[19] Using the symbolic notations $+$ $(-)$ for the entire set of symmetric (antisymmetric) basis functions we have

$$\begin{bmatrix}
\mathcal{M}^{+}_{\mathrm{Ti}}\,|\,\mathcal{M}^{+}_{\mathrm{Ti}} & \mathcal{M}^{+}_{\mathrm{Ti}}\,|\,\mathcal{M}^{+}_{\mathrm{Fe}} & 0 & 0 & \mathcal{M}^{+}_{\mathrm{Ti}}\,|\,h_1 & \mathcal{M}^{+}_{\mathrm{Ti}}\,|\,h_2 \\
\mathcal{M}^{+}_{\mathrm{Fe}}\,|\,\mathcal{M}^{+}_{\mathrm{Ti}} & \mathcal{M}^{+}_{\mathrm{Fe}}\,|\,\mathcal{M}^{+}_{\mathrm{Fe}} & 0 & 0 & \mathcal{M}^{+}_{\mathrm{Fe}}\,|\,h_1 & \mathcal{M}^{+}_{\mathrm{Fe}}\,|\,h_2 \\
0 & 0 & \mathcal{M}^{-}_{\mathrm{Ti}}\,|\,\mathcal{M}^{-}_{\mathrm{Ti}} & \mathcal{M}^{-}_{\mathrm{Ti}}\,|\,\mathcal{M}^{-}_{\mathrm{Fe}} & \mathcal{M}^{-}_{\mathrm{Ti}}\,|\,h_1 & \mathcal{M}^{-}_{\mathrm{Ti}}\,|\,h_2 \\
0 & 0 & \mathcal{M}^{-}_{\mathrm{Fe}}\,|\,\mathcal{M}^{-}_{\mathrm{Ti}} & \mathcal{M}^{-}_{\mathrm{Fe}}\,|\,\mathcal{M}^{-}_{\mathrm{Fe}} & \mathcal{M}^{-}_{\mathrm{Fe}}\,|\,h_1 & \mathcal{M}^{-}_{\mathrm{Fe}}\,|\,h_2 \\
h_1\,|\,\mathcal{M}^{+}_{\mathrm{Ti}} & h_1\,|\,\mathcal{M}^{+}_{\mathrm{Fe}} & h_1\,|\,\mathcal{M}^{-}_{\mathrm{Ti}} & h_1\,|\,\mathcal{M}^{-}_{\mathrm{Fe}} & h_1\,|\,h_1 & h_1\,|\,h_2 \\
h_2\,|\,\mathcal{M}^{+}_{\mathrm{Ti}} & h_2\,|\,\mathcal{M}^{+}_{\mathrm{Fe}} & h_2\,|\,\mathcal{M}^{-}_{\mathrm{Ti}} & h_2\,|\,\mathcal{M}^{-}_{\mathrm{Fe}} & h_2\,|\,h_2 & h_2\,|\,h_2
\end{bmatrix}.$$

There are no matrix elements between functions of different parity. Furthermore, the $\mathcal{M}^{+}\,|\,\mathcal{M}^{+}$ blocks are just the original SK matrix for TiFe (Ref. 19), while the $\mathcal{M}^{-}\,|\,\mathcal{M}^{-}$ blocks are the SK matrix for

$$k=k_0+(2\pi/a,\pi/a,\pi/a)\ .$$

This corresponds to folding (translating) the states at the cubic M point back to the Γ point as noted by Gupta.[14]

Thus, as k_0 ranges over the orthorhombic zone the original cubic zone is sampled. The value $k_x+2\pi/a$ is necessary, for although the Ti | Ti and Fe | Fe blocks are periodic in k_x of cubic (orthorhombic) period $2\pi/a$, the Ti | Fe and Fe | Ti blocks are not, so in order to maintain the correct phases for the second atom in the unit cell with regard to the first, this choice is needed. Thus, one can form the matrix corresponding to the second atom(s) in the unit cell from the first by substituting

$$k=k_0+(2\pi/a,\pi/a,\pi/a) .$$

One can easily derive the matrix elements in the $h_1 \mid \mathcal{M}^{+}_{\mathrm{Ti}}$, $h_1 \mid \mathcal{M}^{+}_{\mathrm{Fe}}$, $h_2 \mid \mathcal{M}^{+}_{\mathrm{Ti}}$, and $h_2 \mid \mathcal{M}^{+}_{\mathrm{Fe}}$ blocks. It again turns out that

$$h_i \mid \mathcal{M}^{-}_{j}(k)=h_i \mid \mathcal{M}^{+}_{j}(k+2\pi/a,\pi/a,\pi/a) ,$$

but because of the locations of the hydrogens one cannot achieve any further simplifications (at arbitrary k) by taking linear combinations $h_1 \pm h_2$. The hydrogens *mix* the cubic states of k and $k=(2\pi/a,\pi/a,\pi/a)$. This matrix now contains an additional ten parameters which describe the H-H, H-Fe, and H-Ti interactions, for a total of 58 parameters. The matrix elements which involve these interactions are given in Table II. In our previous calculations[17] we had made the simplifying decision to freeze the metal-metal parameters to their TiFe values and determine the ten new parameters by fitting them to the three lowest bands of the Gupta's calculations.[14] We have now

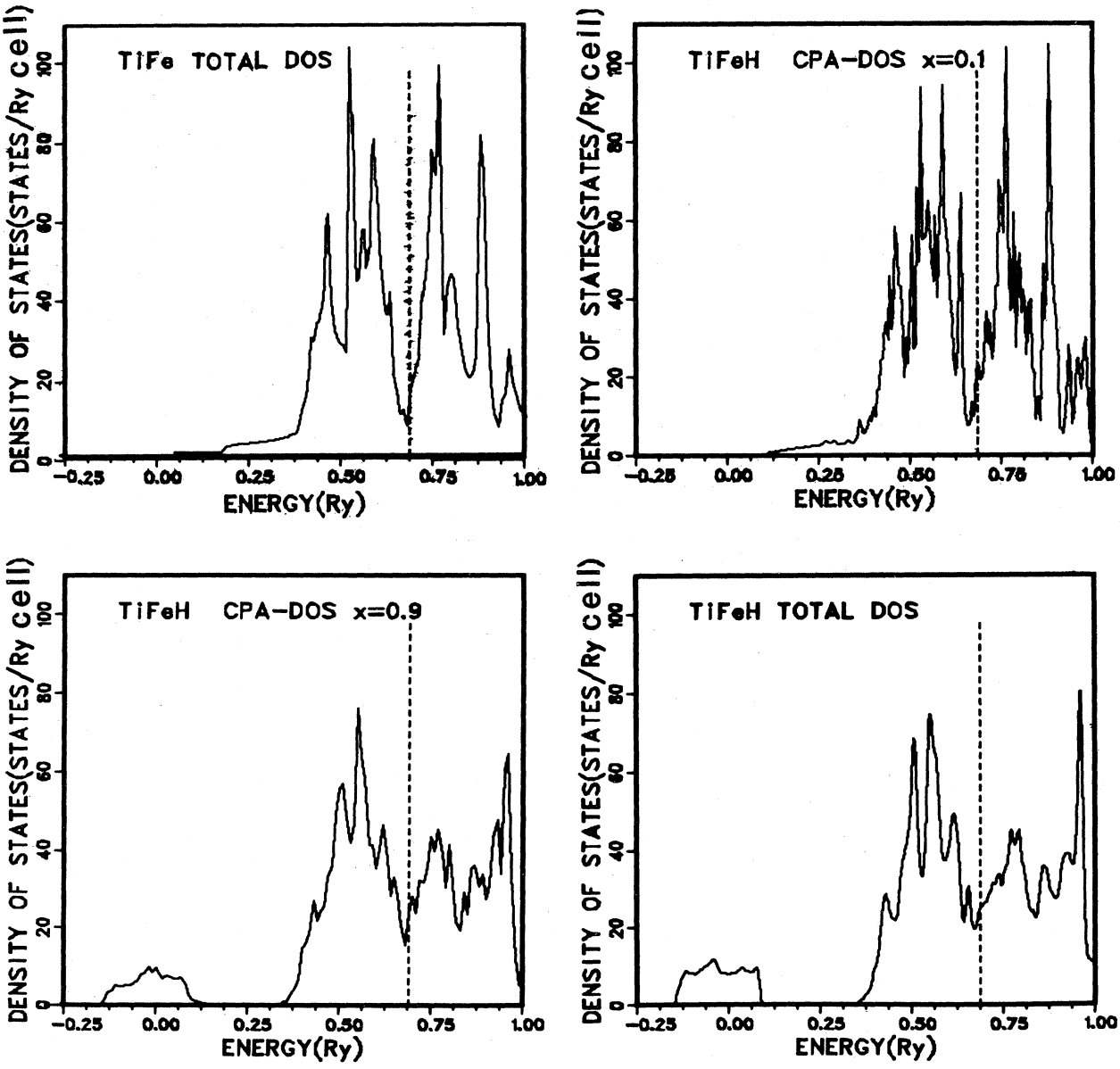

FIG. 1. Total densities of states for TiFeH for $x=0.0$, 0.1, 0.9, and 1.0.

removed this approximation and have determined all the 58 $TiFeH_{1.0}$ parameters by least-squares fitting of 20 bands from Gupta's results. The rms fitting error was less than 20 mRy for 20 bands. The $TiFeH_{1.0}$ SK parameters are listed in Table III. These parameters uniformly shift Gupta's energy bands by 0.137 Ry which align the lower Γ_{12} levels of the TiFe and TiFeH APW calculations and put the two calculations in a common energy scale.

IV. CPA THEORY

The SK Hamiltonian that we have constructed for $TiFeH_{1.0}$ is used in an extension of Faulkner's CPA theory.[15] In this theory it is assumed that the metal sublattice is perfectly periodic while the hydrogen sublattice has random vacant sites. So in our case the effective Hamiltonian is a 38×38 matrix which has a 36×36 block identical to that of the periodic material. In the remaining 2×2 block the on-site SK parameter $E_{h,h}(000)$ is replaced by the self-energy Σ_h which is determined from the CPA condition:

$$xt_{\mathrm{H}}+(1-x)t_v=0\ , \tag{1}$$

where x is the hydrogen concentration, t_{H} and t_v the scattering matrices for hydrogen and vacancy given by the following expressions:

$$t_{\mathrm{H}}=[E_{h,h}(000)-\Sigma_h]\times\{1-[E_{h,h}(000)-\Sigma_h]G_h(z,\Sigma_h)\}^{-1}\ , \tag{2}$$

$$t_v=-[G_h(z,\Sigma_h)]^{-1}\ . \tag{3}$$

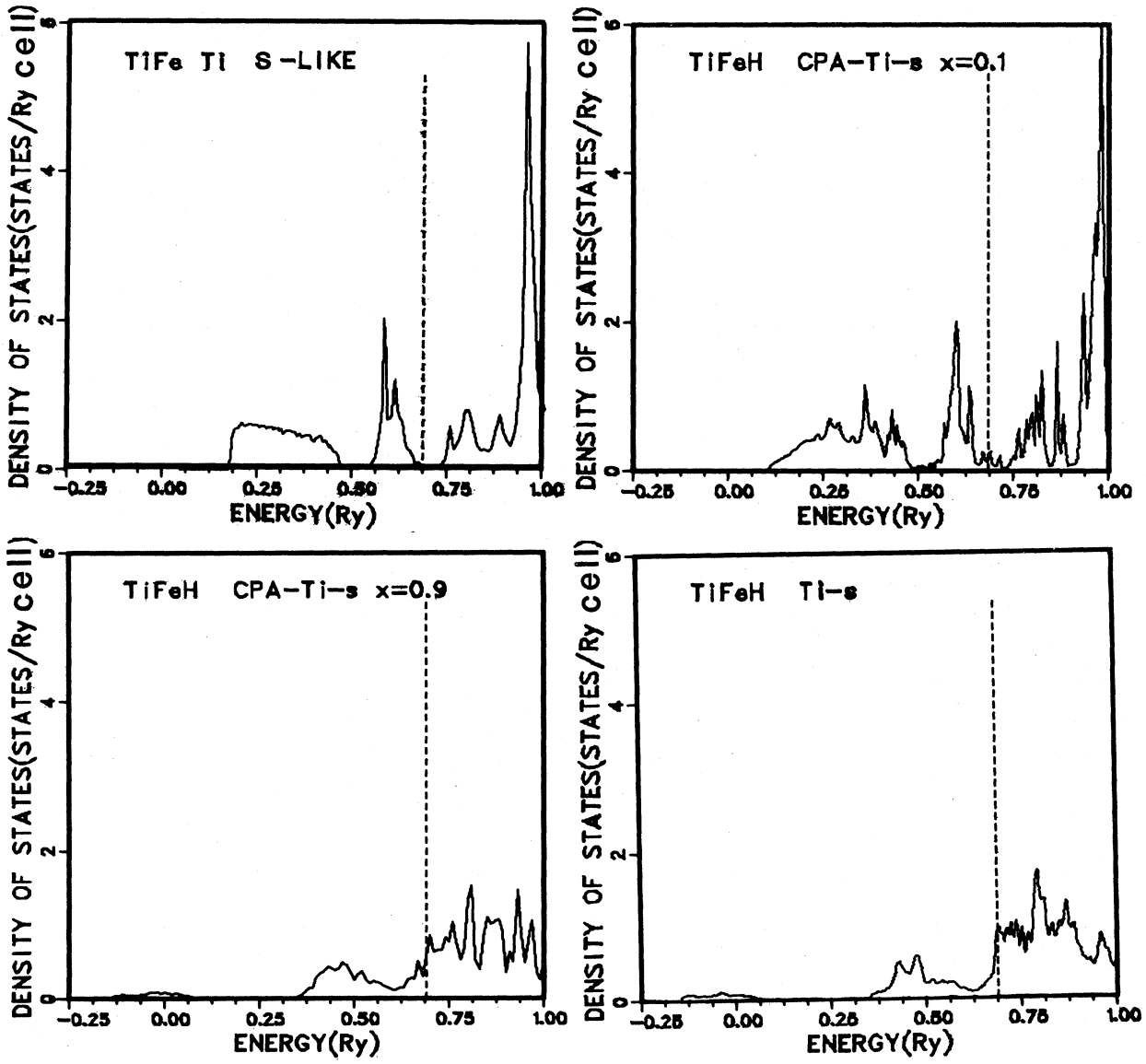

FIG. 2. Titanium s—like component densities of states for compositions as in Fig. 1.

The Green's function $G_h(z,\Sigma_h)$ is the 2×2 block of the 38×38 Green's function $G(z,\Sigma_h)$ that is found by the following integration over the Brillouin zone:

$$G(z,\Sigma_h)=\int_{\mathrm{BZ}}\frac{d^3k}{z-H(k,\Sigma_h)}\ , \tag{4}$$

where z is the complex energy and $H(k,\Sigma_h)$ is the 38×38 effective Hamiltonian in which only diagonal disorder is incorporated through the self-energy Σ_h.

The numerical procedure consists of solving Eqs. (1) and (4) iterating self-consistently to determine Σ_h and $G(z,\Sigma_h)$. The next step is to calculate the DOS from the formula

$$N_l(E)=-\frac{1}{\pi}\lim_{z\to E^+}\mathrm{Im}\,\mathrm{Tr}G_l(E,\Sigma_h)\ , \tag{5}$$

where the index l refers to the s, p, t_{2g}, and e_g symmetries of the Ti, Fe, and hydrogen components. The evaluation of the integral of Eq. (4) requires the inversion of 38×38 matrices at a given energy E, for a large number of k points. We have found that satisfactory convergence occurred using the following procedure: We performed the integration for 175 k points in the entire energy spectrum using an energy interval of 0.01 Ry. This approach provides a reliable determination of the integrated DOS and hence of the Fermi level E_F. However, the values of $N(E_F)$ are far from converged when we use 175 k's. In order to obtain reliable values for $N(E_F)$ we performed the integrations around E_F for a mesh of 4641 k points.

We performed three CPA calculations at $x=0.1$ using for the metal sites the SK parameters of TiFe, and at $x=0.8$ and 0.9 using the SK parameters of $TiFeH_{1.0}$.

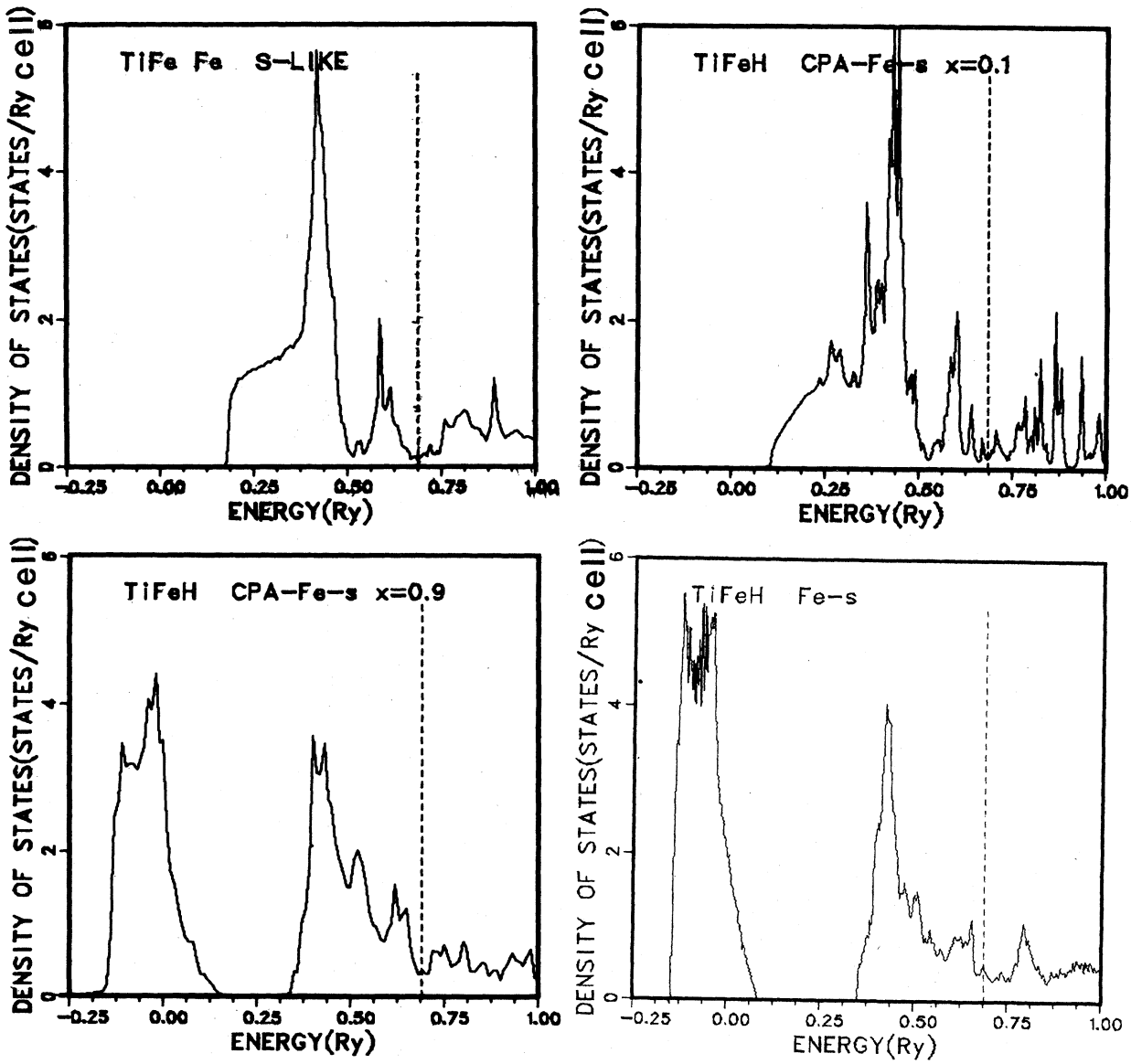

FIG. 3. Iron s—like component densities of states for given compositions.

V. RESULTS AND DISCUSSION

In Figs. 1—11 we present the DOS of two CPA calculations for hydrogen contents $x=0.1$ and 0.9 and compare them with the DOS of TiFe and $TiFeH_{1.0}$. Figure 1 shows the total DOS where we note, for the hydrogen-rich cases ($x=0.9$ and 1.0), that the low-lying hydrogen-induced states are centered at zero of the energy scale. The bonding and antibonding transition-metal states are separated by a minimum in the DOS and the Fermi level E_F lies just above this minimum. The value of this minimum DOS as well as the DOS at E_F increase from TiFe to $TiFeH_{1.0}$ by approximately a factor of 2. In our preliminary paper,[17] although we stressed the nonrigid band characteristics of the hydrogen-metal bonding states, we suggested that E_F increases with increasing x. In the present, more accurate set of calculations, we have found that E_F is very nearly independent of x, near each end of the compositional spectrum, i.e., for $x=0.0$ and 0.1, $E_F=0.67$ Ry and for $x=0.8$, 0.9, and 1.0, $E_F=0.69$ Ry. Our conclusion on this point is similar to that of Temmerman and Pindor[7] in their study of the Pd-Ag-H system. The low-lying hydrogen-induced states are largely of type 1 (i.e., previously occupied) and grow at the expense of the states of mostly iron character. States of type 3 (previously unoccupied) are pulled down below E_F to just accommodate the added electrons with very little readjustment of the Fermi level, but with a concomitant increase of the value of the density of states at the Fermi level.

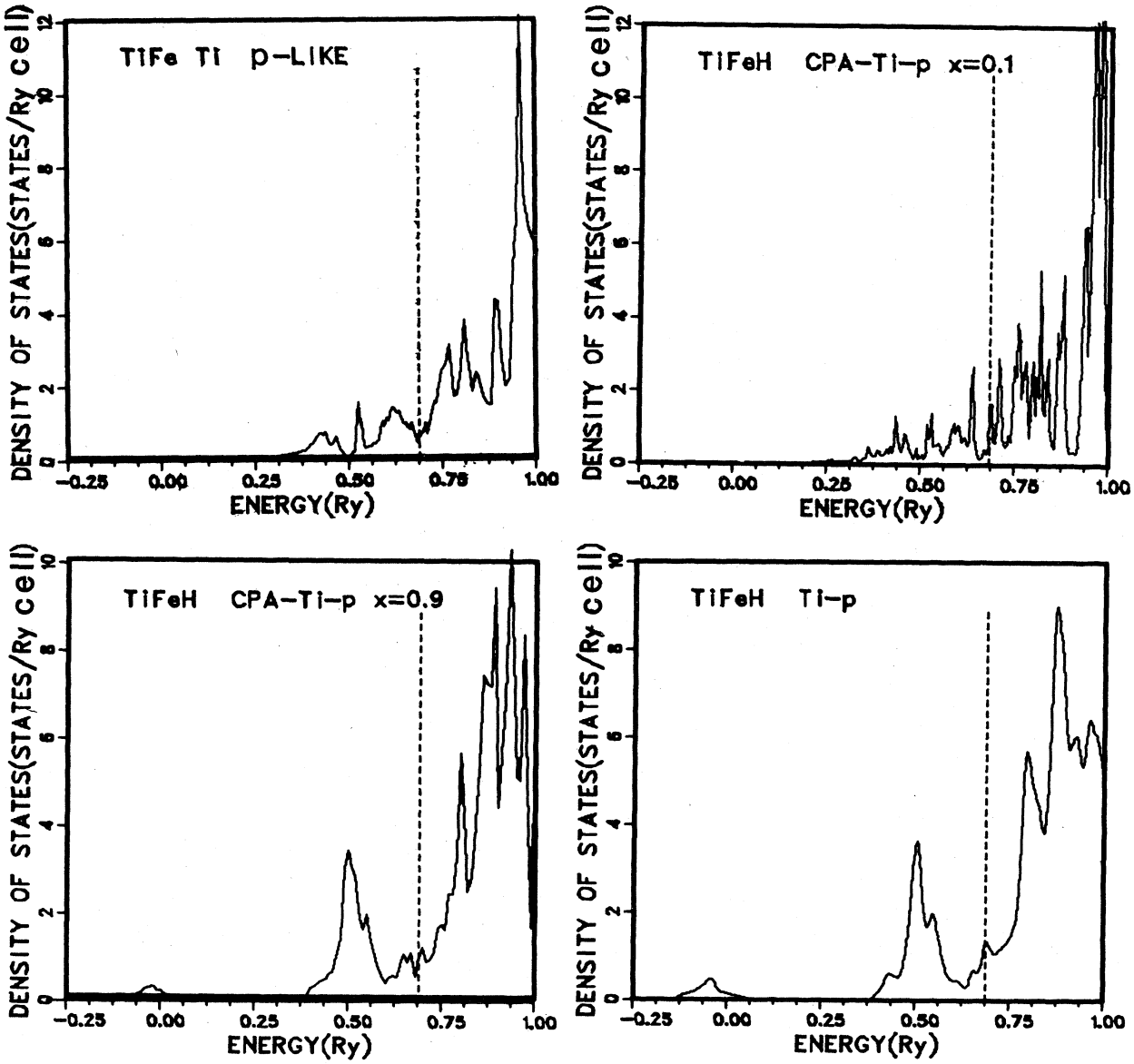

FIG. 4. Titanium p—like component densities of states for stated compositions.

We should point out that the variations of the lattice constant with x are included in our calculations only via the parameters at the two ends of the compositional spectrum. However, we have neglected the small variation of the lattice constant between $x=1.0$ and 0.8, and also between $x=0.0$ and 0.1. In Fig. 2 the s-like DOS for Ti site is shown. The effect of hydrogenation on the Ti s states is that it pushes a small number of states to lower energies but decreases substantially the number of bonding states around 0.3 Ry.

In Fig. 3 the Fe s—like DOS are presented. The effect of hydrogenation now is to split the bonding states into two distinct peaks, one of which is now centered at 0.0 Ry.

In Fig. 4 the Ti p—like DOS are shown. The introduction of large amounts of hydrogen creates again states at low energies and in addition induces a pronounced peak at 0.5 Ry.

The Fe p—like DOS shown in Fig. 5 display again low-lying states induced by the hydrogen presence in the lattice. Also the double peak in the bonding states for $x=0.0$ and 0.1 is replaced by a single broader peak for $x=0.9$ and 1.0.

The Ti d—like DOS are shown in Fig. 6. Besides the appearance of low-lying states for the hydrogen-rich cases the effects of hydrogenation are less pronounced here.

The Fe d—like DOS shown in Fig. 7 indicate a much stronger presence of low-lying states than in other cases. Having decomposed the d DOS into t_{2g} and e_g symmetries we have found that these low-lying states have ex-

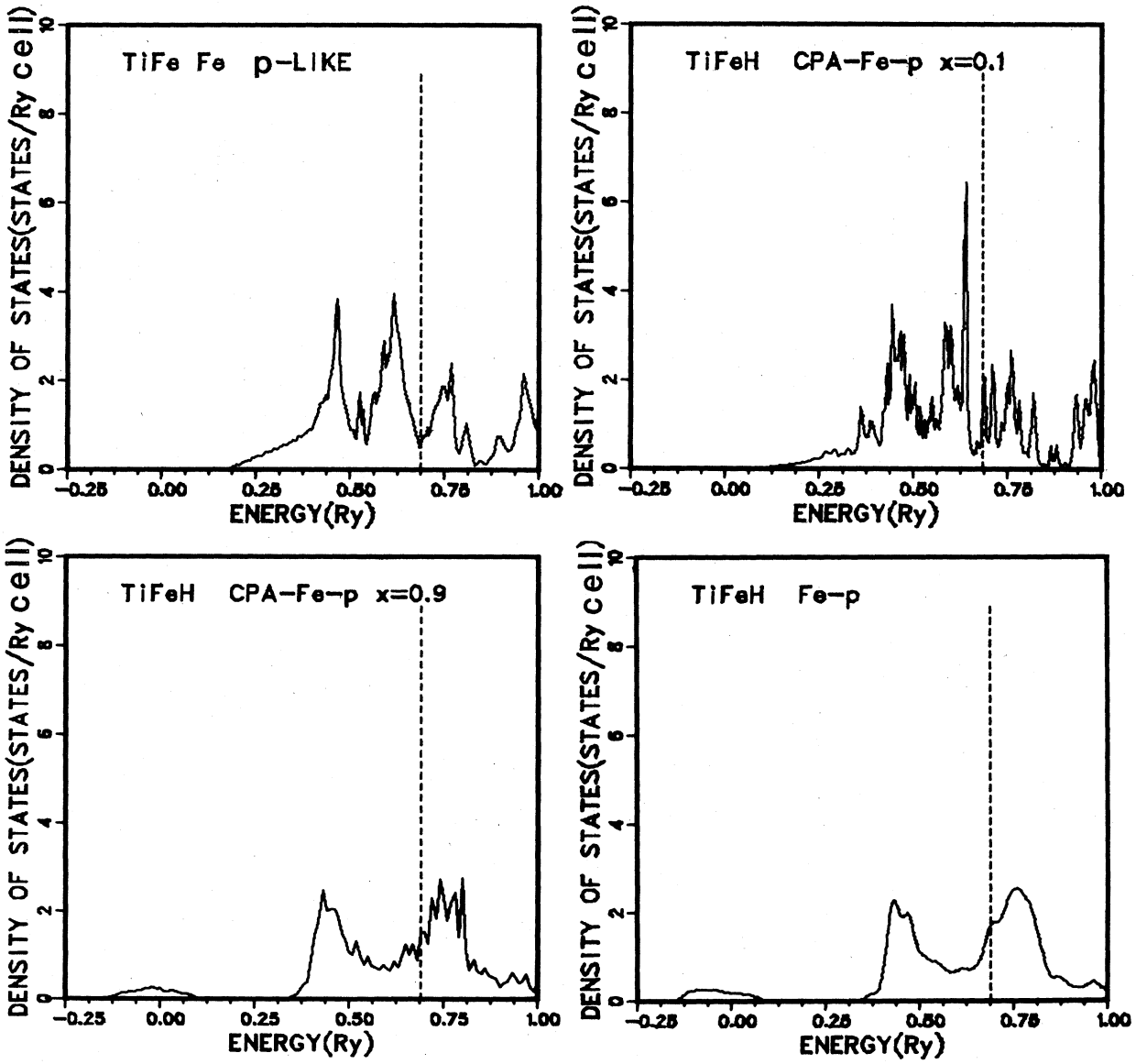

FIG. 5. Iron p—like component densities of states for stated compositions.

clusively e_g symmetry and that they describe the H—Fe bonding. As in the Ti d DOS the rest of the d DOS spectrum remains relatively unchanged.

In Fig. 8 the H-site DOS are shown for $x=0.1$, 0.8, 0.9, and 1.0. We note that the H contribution near E_F is small while the strong hydrogen participation occurs at the low-energy end of the spectrum.

Figure 9 shows the integrated DOS for the low "impurity band" which ends at approximately 0.1 Ry. Looking at the total number of electrons we note a more rapid depletion of states than what a bound state model would predict. For example, at $x=0.8$ our graph shows 1.3 electrons while such predictions give 1.6 electrons. We also note from Fig. 9 that this impurity band mainly consists of Fe s, Fe e_g, and H s, electrons. This implies that H bonds strongly with Fe atoms rather than Ti as might be expected because of its positions between Fe atoms in the lattice. These results also suggest that in the formation of the hydride charge transfer occurs from the H to the Fe sites.

In Fig. 10 the integrated DOS up to E_F is shown. Consistent with our observation that the d states undergo minor modifications upon hydrogenation, we note that the number of d electrons varies slowly with H content. On the other hand, the number of s and p electrons shows a more drastic variation.

The variation of the DOS at E_F, $N(E_F)$, is presented in Fig. 11. The total $N(E_F)$ increases from TiFe to $TiFeH_{1.0}$ by approximately a factor of 3. This is consistent with the measurements of Hempelmann *et al.*[20] who reported a

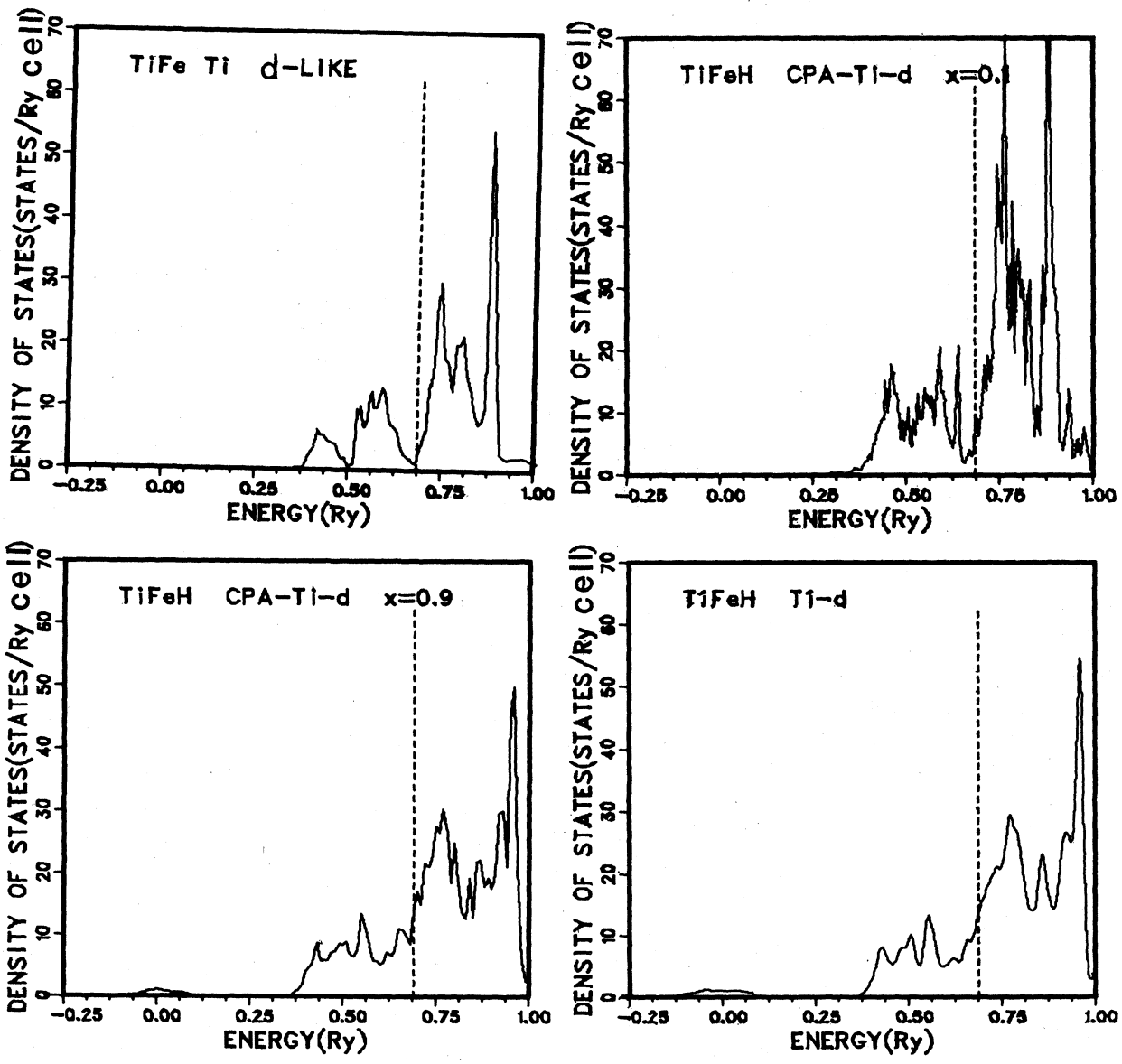

FIG. 6. Titanium d—like component densities of states for stated compositions.

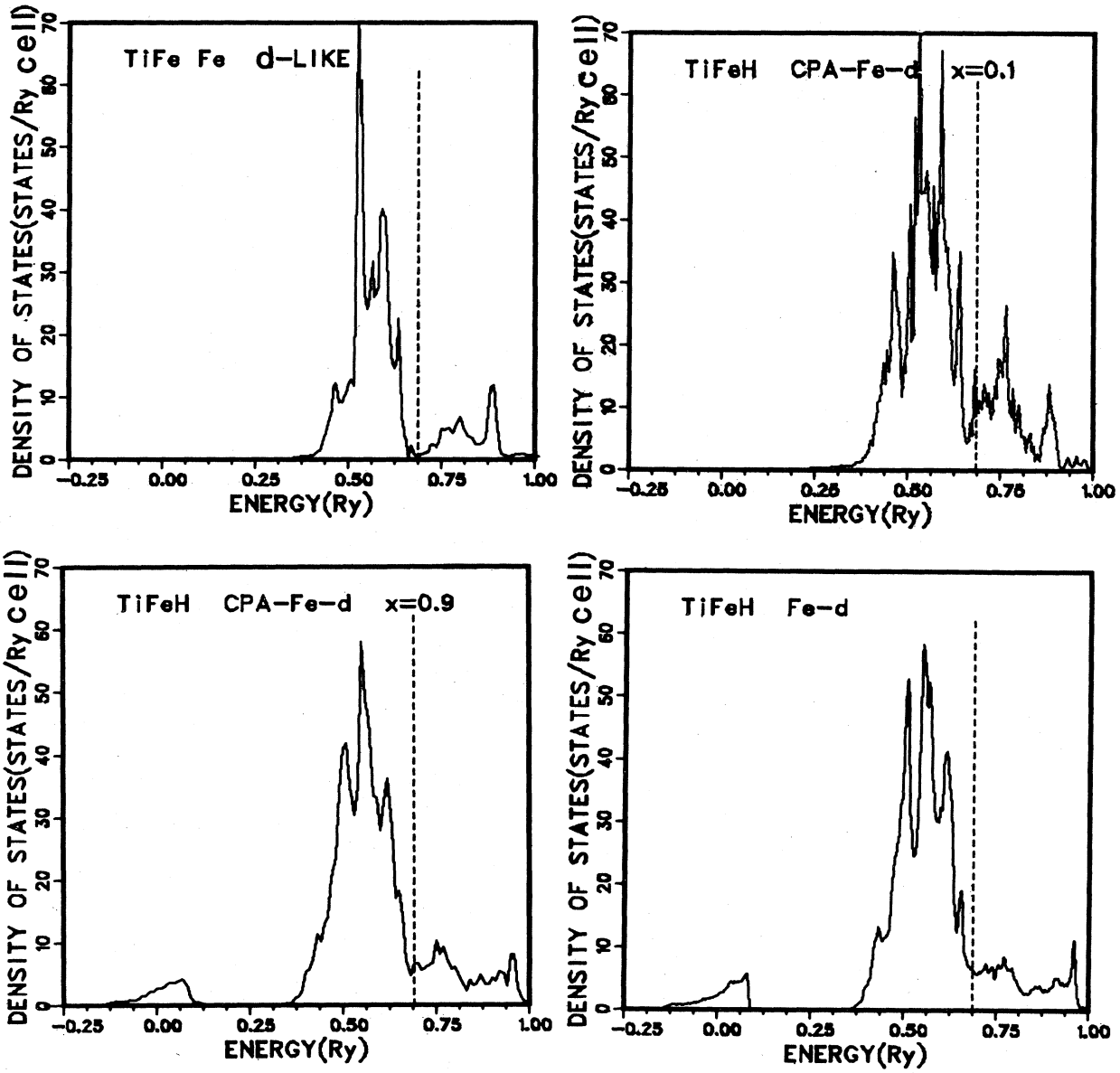

FIG. 7. Iron d—like component densities of states for stated compositions.

rapid increase of the specific heat upon hydrogenation. It is interesting to note from Fig. 11 that while all the other components of $N(E_F)$ increase as a function of x the Fe e_g component decreases.

VI. CONCLUSIONS

Since our calculation at $x=1.0$ is fitted to Gupta's APW results, it is consistent with her conclusions regarding the lowering of states and the introduction of new ones, apart from some quantitative differences due to small errors in fitting and the different ways of obtaining the DOS. We remind the reader that we have assumed in the hydrogen sublattice a random substitution of hydrogen atoms by vacant sites. So in our model the variation of the amount of hydrogen is coupled with the effect of vacancy disorder.

Our main conclusions are that the position of E_F is insensitive to the variation of x but $N(E_F)$ increases rapidly with increasing x. The general shape of the DOS is affected, by changing x, only at low energies where the hydrogen-metal bonding states are located. The effect of disorder can be seen by noting the broadening of the H-site DOS at $x=0.8$. It will be very interesting to examine

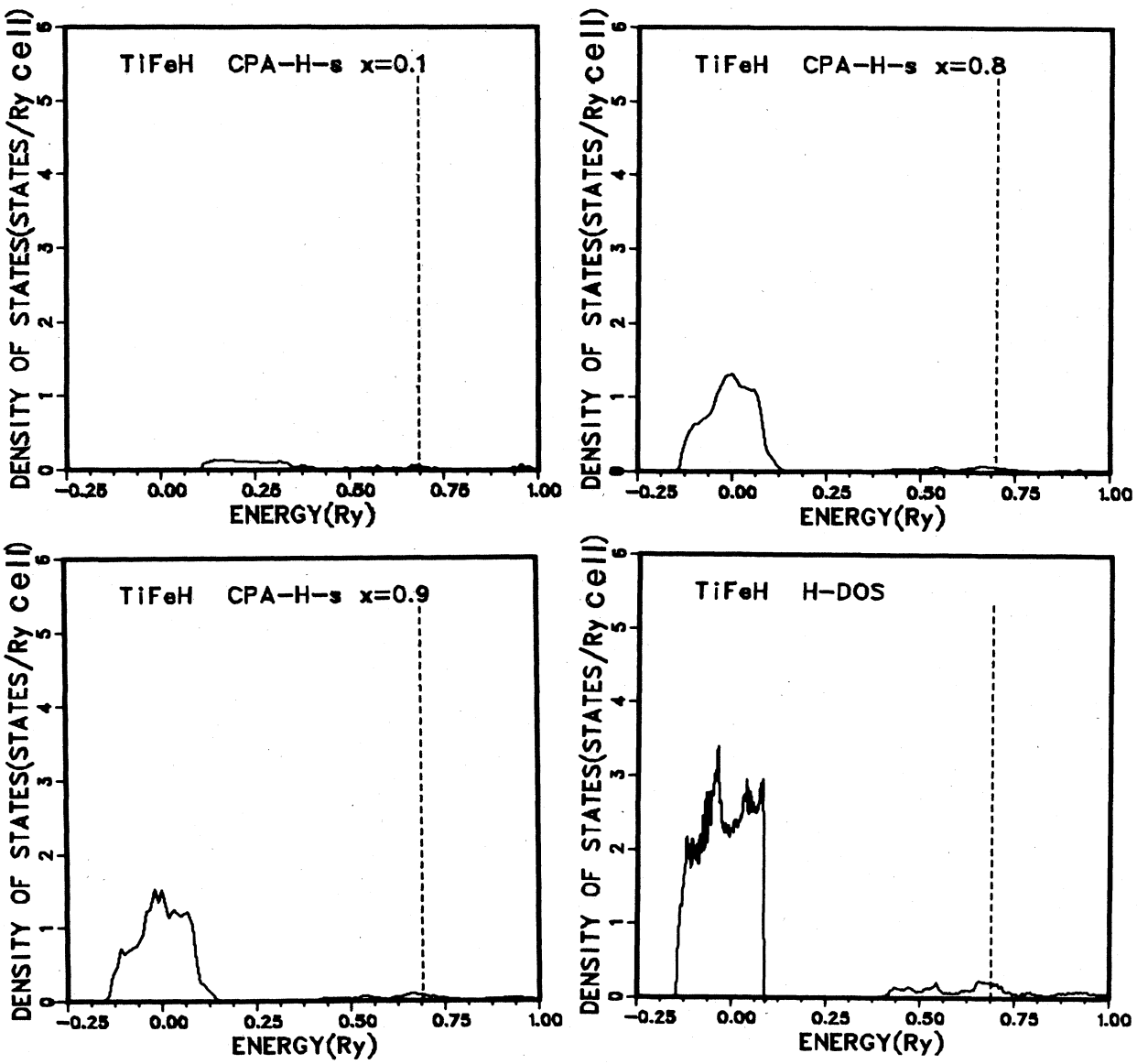

FIG. 8. Hydrogen s—like component densities of states for stated compositions.

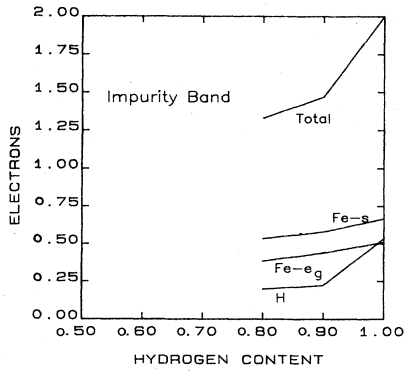

FIG. 9. Character of electrons in the low-lying hydrogen-induced band for the major components.

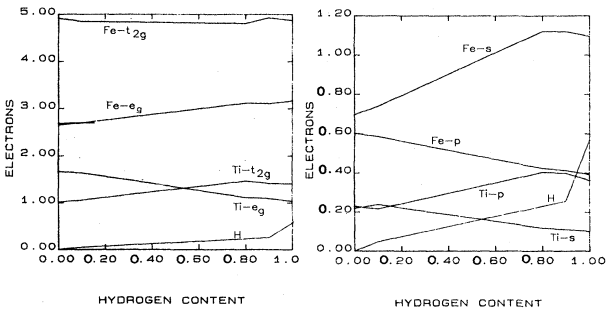

FIG. 10. Variation of the components of the total electron character with composition for the major contributors—left panel, and for the minor contributors—right panel.

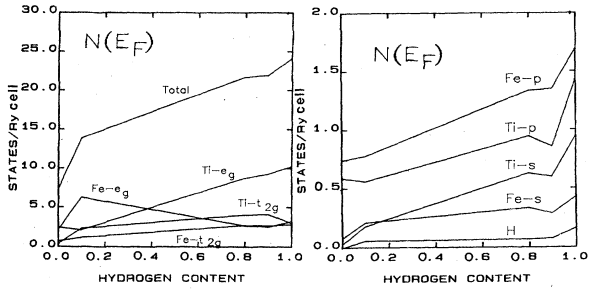

FIG. 11. Variation in the value of the total and component densities of states at the Fermi level with composition: left panel—major contributions, right panel—minor contributions.

the effects of disorder by introducing into our model random substitutions of Ti and Fe atoms in the metal sublattice.

ACKNOWLEDGMENTS

We are indebted and grateful to Dr. Michelle Gupta for copies of unpublished work and numerous helpful discussions. The work performed at Sandia Laboratories was supported by the U.S. Department of Energy under Contract No. DE-AC04-DP00789.

[1]A. C. Switendick, in *Hydrogen in Metals I,* edited by G. Alefeld and J. Völkl [Top. Appl. Phys. **28**, 101 [1978)].

[2]D. A. Papaconstantopoulos, in *Metal Hydrides,* No. 76 of *NATO Advanced Study Institute Series B,* edited by G. Bambakidis (Plenum, New York, 1981), pp. 215-242.

[3]M. Gupta, *Metal Hydrides,* No. 76 of *NATO Advanced Study Institute Series B,* edited by G. Bambakidis (Plenum, New York, 1981), pp. 255–272.

[4]C. D. Gelatt, Jr., H. Ehrenreich, and J. Weiss, Phys. Rev. B **17**, 1940 (1978).

[5]A. C. Switendick, J. Less-Common Met. **101**, 191 (1984).

[6]C. T. Chan and S. G. Louie, Phys. Rev. B **27**, 3325 (1983).

[7]W. M. Temmerman, and A. J. Pindor, J. Phys. F **13**, 1627 (1983); A. J. Pindor, W. M. Temmerman, and B. L. Gyorffy, *ibid.,* F **13**, 1869 (1983).

[8]J. J. Reilly, Jr., Z. Phys. Chem. Neue Folge **117**, 155 (1979).

[9]A. R. Miedema, J. Less-Common. Met. **32**, 117 (1973); P. C. Bonten and A. R. Miedema, J. Less-Common Met. **71**, 147 (1980).

[10]C. E. Lundin, F. E. Lynch, and C. B. McGee, J. Less-Common Met. **56**, 19 (1977).

[11]D. G. Westlake, in *Metal Hydrides,* No. 76 of *NATO Advanced Study Institute Series B,* edited by G. Bambakidis (Plenum, New York, 1981), pp. 145–176.

[12]P. Soven, Phys. Rev. **156**, 809 (1967).

[13]D. A. Papaconstantopoulos, Phys. Rev. B **11**, 4801 (1975).

[14]M. Gupta, J. Phys. F **12**, L57 (1982); Phys. Lett. **88A**, 469 (1982).

[15]J. S. Faulkner, Phys. Rev. B **13**, 2391 (1976).

[16]D. A. Papaconstantopoulos, B. M. Klein, J. S. Faulkner, and L. L. Boyer, Phys. Rev. B **18**, 2784 (1978).

[17]D. A. Papaconstantopoulos and A. C. Switendick, J. Less-Common. Met. **88**, 273 (1982).

[18]J. C. Slater and G. F. Koster, Phys. Rev. **94**, 1498 (1954).

[19]J. D. Shore and D. A. Papaconstantopoulos, J. Phys. Chem. Solids **45**, 439 (1984).

[20]R. Hempelmann, D. Ohlendorf, and E. Wicke, in *Hydrides for Energy Storage,* proceedings of an International Symposium, Geilo, Norway, edited by A. F. Andresen and A. J. Maeland (Pergamon, New York, 1977), p. 407.